



# Acoustic Green's functions using the Sinc-Galerkin method

Adrian R.G. Harwood<sup>1</sup>; Iain D.J. Dupère<sup>2</sup>

School of Mechanical, Aerospace & Civil Engineering  
The University of Manchester  
Sackville Street  
Manchester  
M1 3BB, United Kingdom

## ABSTRACT

Green's functions represent the scattering behaviour of a particular geometry and are required to propagate acoustic disturbances through complex geometries using integral methods. The versatility of existing integral methods of acoustic propagation may be greatly increased by using numerical Green's functions computed for more general geometries. We investigate the use of the Sinc-Galerkin method to compute Green's functions for the Helmholtz equation subject to homogeneous Dirichlet boundary conditions. We compare the results to a typical boundary element method implementation. The Sinc-Galerkin procedure demonstrates improved performance on a number of configurations tested in comparison to the BEM. In particular, accuracy comparable to BEM can be achieved in far less time while being less sensitive to both frequency and source position, although the BEM captures the tip of the singularity more completely. The characteristic exponential convergence, as expected, is slower than many Sinc-Galerkin applications due to the presence of the domain singularity typical of Green's functions.

Keywords: Sinc-Galerkin, Boundary Value Problem, Green's Functions

I-INCE Classification of Subjects Number(s): 23.6

## 1. INTRODUCTION

The noise associated with engineering products can be a source of annoyance, distraction or indeed a hazard to health. In particular, motivated by the increase in jet air travel in the 1950s, there has been a focussed effort on developing mathematical means of describing the mechanism of noise generation associated with unsteady fluid flow (aero-acoustic noise). This description together with a means of describing the propagation and scattering of the noise by solid or fluid boundaries allows us to predict noise emission and design quieter products in the future.

One prominent achievement has been the development of a range of noise prediction schemes which make use of numerical methods, analytical models, or a combination of both, to calculate both the hydrodynamic and acoustic pressure fields from a source region all the way to an observer location. The particular class of acoustic prediction schemes known as hybrid schemes use a combination of numerical techniques and analytical formulae to compute an aero-acoustic source and propagate it to an observer, usually many wavelengths away. Use of these schemes as an alternative to solely numerical procedures precludes the need to mesh and solve equations in the extensive region between the source and the observer meaning the demand on computational resources is significantly less. More information on hybrid noise prediction schemes may be found in Wang *et al.* [1].

Hybrid schemes generally rely on the evaluation of an integral equation for the propagation step whose kernel consists of a Green's function. This Green's function often satisfies the boundary conditions in the propagation domain. Physically, this Green's function encapsulates all the complex interactions of the source as the radiation propagates from a particular source location to a particular observer location. Therefore, the Green's function is a powerful representation which, when convoluted with a description of the source, may be used to yield the observed acoustic field in a single

---

<sup>1</sup>adrian.harwood@manchester.ac.uk

<sup>2</sup>iain.dupere@manchester.ac.uk

integration. Analytical representations of Green's functions are few and far between, and are generally approximations [2]. Hence, we are limited to propagating sound using integral equations in regions where Green's functions are available.

In order to extend the versatility of existing hybrid CAA schemes, we develop here a procedure suitable for computing the Green's function for time harmonic acoustic problems. The inclusion of this procedure in a domain decomposition algorithm will allow the accurate and robust computation of acoustic Green's functions in geometries where analytical representations are unavailable. Alternatively, the method may be used to compute Green's functions for periodic domains.

### 1.1 Sinc Methods

The set of Sinc numerical methods represent the function of interest as an expansion of translated Sinc functions. Recently this basis has been used as part of practical spatial/spectral methods for the solution of elliptic and parabolic linear and non-linear differential equations by Stenger [3]. Stenger demonstrates that for appropriately selected discretisation parameters, the unique properties of the Sinc basis ensure exponential convergence of the Sinc series representation.

In one dimension, the Sinc basis functions exist along the whole real line, centred at uniformly distributed Sinc nodes. This infinite interval, and the functions and nodes within the space, may be transformed to any semi-infinite or finite interval through conformal mapping. This allows functions on an arbitrary 1D interval, as well as their integrals and derivatives, to be approximated using an expansion of the transformed Sinc functions centred at the transformed nodal locations in the interval. For many practical problems, such as the ones presented in this paper, the solution in the domain is assumed unknown. The coefficients of the Sinc functions may then be found using a collocation [4] or Galerkin [5] procedure. The collocation method is generally chosen over the Galerkin method for problems with variable coefficients as the resulting implementation is a more efficient means of achieving a given accuracy. Despite this benefit, the Galerkin procedure is more flexible as it lends itself to basis modification and extension without the stringent smoothness requirements of the collocation method [6] and so is used here. A rigorous mathematical summary of the Sinc method formulae can be found in Lund & Bowers [7].

### 1.2 Advantages of Sinc-Galerkin

An important practical advantage of using spectral-like methods over other numerical methods such as the boundary element method (BEM) is that once the coefficients have been found, the evaluation of points within and on the domain boundaries requires simply the evaluation and assembly of the series components. We compare our Sinc implementation to a typical BEM implementation in Section 5, where the issue of re-evaluating coefficient matrices for every internal point is seen to significantly impact execution time.

The principal advantage of the Sinc-Galerkin method over Galerkin methods with different basis functions is the ability to achieve exponential convergence of the series solution. This behaviour has been established for a number of problems in the literature, even for those featuring a boundary singularity [8]. However, the method has not been applied to a BVP featuring a domain singularity, such as the one we present here. Additional advantages of the Sinc-Galerkin approach when compared with alternative numerical methods are described elsewhere [5, 8].

The merits of the Sinc-Galerkin method have led to its applications to both 1D and higher-dimensional problems. The combination of Sinc methods with Dirichlet conditions is relatively straight-forward since the Sinc function satisfies the homogeneous Dirichlet condition automatically. A simple change of variable is all that is required for the conversion of the problem with inhomogeneous conditions to the problem with homogeneous conditions (see Lund & Bowers [7]).

As the developments below illustrate, Sinc methods, like wavelet methods, are limited (in their direct application) to rectangular or rectangular parallelepiped infinite, semi-infinite or finite geometries. This is ideal for treating problems with periodic boundary conditions. Attempts to extend Sinc-Galerkin and similar procedures to more complex geometries either transform the problem as recommended by McArthur *et al.* [8] or use a sub-domain ('building-block') approach [9].

## 2. GREEN'S FUNCTION FOR THE HELMHOLTZ EQUATION

Time-harmonic acoustic problems, in the absence of a mean flow, may be represented by a Dirichlet Helmholtz BVP of the form

$$(\nabla^2 + k^2)u(\mathbf{x}, \omega) = f(\mathbf{x}, \omega) \quad \text{in } \Omega \quad (1a)$$

$$u(\mathbf{x}, \omega) = g(\omega) \quad \text{on } \partial S \quad (1b)$$

This BVP physically describes an acoustic source  $f$  radiating sound at a given frequency  $\omega$  into the domain where the resulting acoustic fluctuations are governed by the linear wave equation and are equal to  $g$  on the domain boundary. In the most general case we assume the source term to be a function of spatially compact support. One method of developing an analytical solution to this BVP is to transform the differential equation into an integral equation in which we can substitute the boundary conditions. These boundary conditions are incorporated in the integral kernel through the Green's function  $\hat{G}(\mathbf{x}, \mathbf{y}, \omega)$ , where  $\mathbf{y}$  refers to the spatial coordinate of the compact source function, and  $\mathbf{x}$  the observer coordinate. This function represents the outgoing wave produced by an impulsive unit point source at  $\mathbf{y}$  subject to the same boundary conditions as the original problem. It is the solution to the singular form of the original BVP, where the source is described by the Dirac delta function (Equation (2)).

$$(\nabla^2 + k^2)\hat{G}(\mathbf{x}, \mathbf{y}, \omega) = \delta(\mathbf{x} - \mathbf{y}) \quad \text{in } \Omega \quad (2a)$$

$$\hat{G}(\mathbf{x}, \mathbf{y}, \omega) = g(\mathbf{y}, \omega) \quad \text{on } \partial S \quad (2b)$$

In the absence of boundary conditions we may consider this wave to propagate in free-space and hence we often use the free-space Green's function, readily available in analytical form [2], to solve the problem. However, the introduction of boundaries and hence associated boundary conditions complicate matters as an analytical representation of  $\hat{G}$  is difficult to construct. In the remainder of this paper we show that the Sinc-Galerkin method can be a robust and accurate means of numerically computing Green's functions for homogeneous Dirichlet Helmholtz BVPs within a particular class of geometries.

### 3. 1D SINC APPROXIMATIONS

We start by presenting the key formulae associated with Sinc numerical methods before extending them to our particular application. The one-dimensional Sinc approximation for a function  $f(x)$  on the real line  $x \in \mathbb{R}$  may be defined for step size  $h > 0$  as

$$f(x) \approx \sum_{k=-M}^N f(kh) \text{sinc}\left(\frac{x - kh}{h}\right) \quad (3)$$

where

$$\text{sinc}(z) \equiv \begin{cases} \frac{\sin(\pi z)}{\pi z} & z \neq 0 \\ 1 & z = 0 \end{cases}$$

Since  $\text{sinc}\left(\frac{x - kh}{h}\right) = 1$  when  $x = kh$ , this approximation interpolates  $f$  at the collocation points  $\{nh\}_{n=-\infty}^{\infty}$ . Integration of the series representation over the whole the real line defines the 1D quadrature rule

$$\int_{-\infty}^{\infty} f(x) dx \approx h \sum_{k=-M}^N f(kh) \quad (4)$$

When using these approximate formulae, it is important to select the truncation and step parameters such that the error in the approximation behaves exponentially. This ensures the series representation remains rapidly convergent. Accurate approximations may then be achieved using a relatively small number of terms in the series. This is a particular strength of Sinc series representations over similar representations such as Fourier series. The mathematical rules for parameter selection are established for a number of problems in the textbook [7], although in all cases, knowledge of the solution behaviour at the endpoint of the interval is required. In practice, such information is rarely available and hence a set of 'general' selections are made when performing our calculations which are

detailed later.

For many boundary value problems, the domain boundaries are finite, and Equation (3) may be mapped from  $x \in \mathbb{R}$  to the interval  $x' \in [a, b]$  using the conformal mapping function  $\phi : x \mapsto x'$  defined by

$$\phi(x) = \ln \left( \frac{x-a}{b-x} \right) \quad (5)$$

If the inverse mapping function is defined by  $\psi(x') = \phi^{-1}(x')$  then we have the new composite interpolation formula for the interval  $[a, b]$  as

$$f(x) \approx \sum_{k=-M}^N f \circ \psi(kh) [S(k, h) \circ \phi(x)] \quad (6)$$

as well as the new quadrature formulation

$$\int_a^b f(x) dx \approx h \sum_{k=-M}^N \frac{f}{\phi'} \circ \psi(kh) \quad (7)$$

where we have used a shorthand notation for a translated sinc function defined by

$$S(k, h)(z) \equiv \text{sinc} \left( \frac{z - kh}{h} \right) \quad (8)$$

Finally, as many differential equations contain derivatives we also define the following [10]

$$\delta_{jk}^{(n)} \equiv h^n \frac{d^n}{d\phi^n} [S(j, h) \circ \phi(x)] \Big|_{x=x_k} \quad n = 0, 1, 2, \dots \quad (9)$$

where  $x_k = \phi^{-1}(kh) = \psi(kh)$ . The values of  $\delta_{jk}^{(n)}$  may be found by observing  $\phi(x_k)|_{x=x_k} = \phi(\phi^{-1}(kh)) \equiv x|_{x=kh}$  and

$$\frac{d^n}{d\phi^n} [S(j, h) \circ \phi(x)] \Big|_{x=x_k} = \frac{d^n}{dx^n} \left[ \text{sinc} \left( \frac{x - jh}{h} \right) \right] \Big|_{x=kh}$$

Next we introduce the Sinc-Galerkin procedure for a two-dimensional Helmholtz BVP and show the simple extension of the formulae presented in this section to two dimensions.

#### 4. 2D SINC-GALERKIN FOR THE HELMHOLTZ EQUATION

The 2D Sinc-Galerkin method for a homogeneous Dirichlet BVP may be derived by considering the Helmholtz equation on a rectangle  $(a, b) \times (c, d)$  subject to homogeneous Dirichlet conditions on the edges (Equation (10)).

$$(\nabla^2 + k^2)u(x, y) = -f(x, y) \quad (x, y) \in \Omega = (a, b) \times (c, d) \quad (10a)$$

$$u(x, y) = 0 \quad (x, y) \in \partial\Omega \quad (10b)$$

Extending Equation (7) to two dimensions we may approximate the solution to Equation (10) as a sinc series

$$u_A(x, y) = \sum_{j=-M_x}^{N_x} \sum_{k=-M_y}^{N_y} u_{jk} S_{jk}(x, y) \quad (11)$$

In this case, the coefficients at the nodal points of each sinc function in the basis set are unknown since the solution itself is unknown. These unknown are represented by the coefficients  $u_{jk}$ . The basis functions  $\{S_{jk}(x, y)\}$  use the shorthand of Equation (8) defined

$$S_{jk}(x, y) = [S(j, h_x) \circ \phi_x(x)] [S(k, h_y) \circ \phi_y(y)] \quad (12)$$

The required mapping function for the  $x$ -direction and  $y$ -direction are given by

$$\phi_x(x) = \ln \frac{x-a}{b-x} \quad \phi_y(y) = \ln \frac{y-c}{d-y}$$

We initiate the Galerkin method by considering the orthogonalisation of the residual  $R = -(\nabla^2 + k^2)u_A - f$  with respect to the original basis set of functions Equation (12) using a weighting function  $w(x)v(y) = 1/\sqrt{\phi'_x(x)\phi'_y(y)}$ . This selection of weighting function ensures the boundary terms generated by the inner products are equal to zero. The weighted residual statement is then discretised by substituting the 2D approximation  $u_A$  and applying the 2D quadrature rule

$$\iint z(x,y) dx dy \approx h_x h_y \sum_{j=-M_x}^{N_x} \sum_{k=-M_y}^{N_y} \frac{z(x_j, y_k)}{\phi'_x(x_j)\phi'_y(y_k)}$$

which is equivalent to Equation (7) extended to two dimensions, where  $z(x,y)$  is an arbitrary 2D function and the nodal points are represented by combinations of  $(x_j, y_k)$ . The result is the following discretised equation for a given combination of basis functions

$$\begin{aligned} \frac{v}{\phi'_y(y_q)} \sum_{j=-M_x}^{N_x} \left[ -\frac{1}{h_x^2} \delta_{pj}^{(2)} \phi'_x w - \frac{1}{h_x} \delta_{pj}^{(1)} \left( \frac{\phi''_x}{\phi'_x} w + 2w' \right) - \delta_{pj}^{(0)} \frac{w''}{\phi'_x} \right] (x_j) u_{jq} \\ + \frac{w}{\phi'_x(x_p)} \sum_{k=-M_y}^{N_y} \left[ -\frac{1}{h_y^2} \delta_{qk}^{(2)} \phi'_y v - \frac{1}{h_y} \delta_{qk}^{(1)} \left( \frac{\phi''_y}{\phi'_y} v + 2v' \right) - \delta_{qk}^{(0)} \frac{v''}{\phi'_y} \right] (y_k) u_{pk} \\ - k^2 \frac{vw}{\phi'_x \phi'_y} (x_p, y_q) u_{pq} = \frac{f v w}{\phi'_x \phi'_y} (x_p, y_q) \end{aligned} \quad (13)$$

Allowing  $p$  and  $q$  to vary over their range of values we generate a system of equations which after some slight rearrangement can be expressed as

$$\mathbf{D}(\phi'_x) \tilde{\mathbf{A}}(w) \mathbf{D}(\phi'_x) \mathbf{V} + \mathbf{V} \left[ \mathbf{D}(\phi'_y) \tilde{\mathbf{A}}(v) \mathbf{D}(\phi'_y) \right]^T - k^2 \mathbf{V} = \mathbf{G}$$

where  $\mathbf{D}$  represents a diagonal matrix and

$$\begin{aligned} \tilde{\mathbf{A}}(\omega) &= -\frac{1}{h^2} \mathbf{I}^{(2)} - \frac{1}{h} \mathbf{I}^{(1)} \mathbf{D} \left( \frac{\phi''}{(\phi')^2} + \frac{2\omega'}{\phi'\omega} \right) - \mathbf{D} \left( \frac{\omega''}{(\phi')^2 \omega} \right) \\ \mathbf{V} &= \mathbf{D}(w) \mathbf{U} \mathbf{D}(v) \\ \mathbf{G} &= \mathbf{D}(w) \mathbf{F} \mathbf{D}(v) \end{aligned} \quad (14)$$

where  $\omega$  can be either  $v$  or  $w$  and the elements of the matrices  $\mathbf{I}^{(n)}$  are evaluated using Equation (9). Using the definitions  $\mathbf{D}(\phi'_x) \tilde{\mathbf{A}}(w) \mathbf{D}(\phi'_x) = \mathbf{A}_x$  and  $\mathbf{D}(\phi'_y) \tilde{\mathbf{A}}(v) \mathbf{D}(\phi'_y) = \mathbf{A}_y$  we represent this system as a generalised Sylvester equation

$$(\mathbf{A}_x - k^2 \mathbf{I}_{m_x}) \mathbf{V} + \mathbf{V} \mathbf{A}_y^T = \mathbf{G} \quad (15)$$

$\mathbf{I}_{m_x}$  is here an identity matrix of size  $m_x \times m_x$ .

#### 4.1 Parameter Selection

The optimum choice of  $M_x$  and  $N_x$  depends on the behaviour of the solution at the boundaries of the interval. Suitable choices enhance the convergence rates of the method as the theorems of [7] illustrate. However, for practical problems, the solution is likely unknown and hence we use the advice of Mueller and Shores [11] to make sensible selections. From this paper we know

$$N = \left\lceil \left\lfloor \frac{\alpha}{\beta} M + 1 \right\rfloor \right\rceil \quad h = \sqrt{\frac{\pi d}{\alpha M}}$$

and we also choose  $\alpha = \beta = 1$ . In addition, we use the conservative choice of  $d = \pi/4$ .

## 5. NUMERICAL VALIDATION

We now apply the 2D Sinc-Galerkin formulation to compute Green's functions within a rectangular patch subject to homogeneous Dirichlet-type boundary conditions ( $g = 0$  in Equation (1)). Although we choose to compute Green's functions for the Helmholtz equation, the formulation presented here may be used also for Laplace's equation without significant modification. We provide the analytical solution for the example below which we use as a means of assessing the accuracy of our results. Furthermore, the speed of computation is assessed by comparing the results to those obtained using a constant-element direct BEM implementation. The extension of the present formulation to 3D is straightforward [7] but is not performed here for brevity.

As a means of examining convergence we vary the mesh density uniformly up to a maximum of 3 times the lowest mesh density in order to show the trend. We also compare the results to those computed using a direct-collocation BEM implementation over a range of mesh densities. As before, the ratio between the largest and smallest mesh density is 3. In addition, we record the time taken to execute the code in both cases. All computations are performed on an Intel Core i7 870 CPU.

### 5.1 Source Specification

In order to configure the Sinc-Galerkin method for our problems (Equation (1)), we must specify a suitable source function  $f$ . As we are considering the BVP defined by Equation (2) along with homogeneous boundary conditions, analytically, the source function is equal to the Dirac delta function centred at  $(y_1, y_2)$ . We exploit the sifting property to express the source inner product analytically avoiding any potential error introduced by an approximation. Using the coordinate definition of the previous section and denoting the source location in the rectangle by  $(x_0, y_0)$  we have

$$\begin{aligned} \langle f, S_{pq} \rangle &= \iint_{\Omega} \delta(x - x_0) \delta(y - y_0) [S(p, h_x) \circ \phi_x(x)] [S(q, h_y) \circ \phi_y(y)] dx dy \\ &= S_{pq} vw(x_0, y_0) \end{aligned}$$

which is included in Equation (13) as

$$f_{pq}(x_0, y_0, x_p, y_q) \equiv \frac{1}{h_x h_y} [S_{pq} vw](x_0, y_0) \left[ \frac{vw}{\phi'_x \phi'_y} \right] (x_p, y_q)$$

### 5.2 Green's Function for the 2D Helmholtz equation

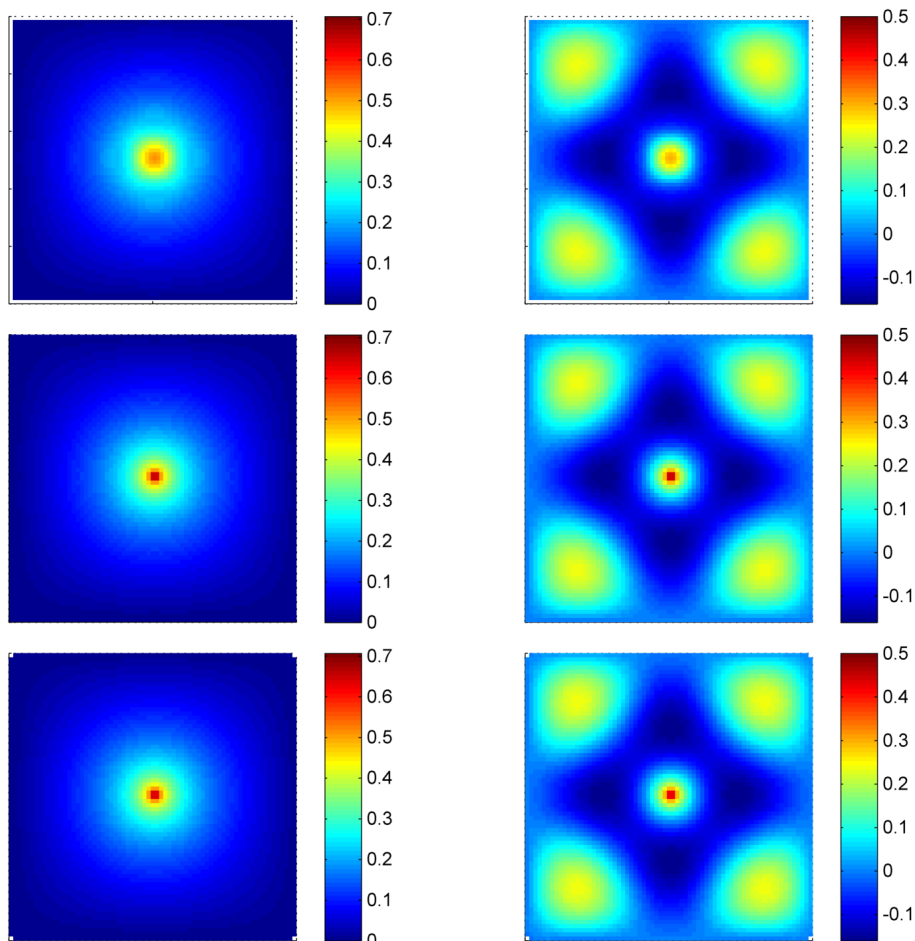
We consider the Green's function for the Helmholtz equation in a rectangle subject to homogeneous Dirichlet boundary conditions on the walls (Equation (2) with  $g = 0$ ). The analytical solution to the problem may be constructed using a double Fourier sine transform method [12] giving, for a source of magnitude  $f_0$ , located at  $(\eta_0, \xi_0)$ , in the rectangle ( $a \times b$ ) for wave number  $k$

$$u(x, y) = \frac{4f_0}{ab} \sum_{n=1}^{\infty} \sum_{m=1}^{\infty} \left[ \frac{\sin\left(\frac{n\pi x}{a}\right) \sin\left(\frac{m\pi y}{b}\right) \sin\left(\frac{n\pi\eta_0}{a}\right) \sin\left(\frac{m\pi\xi_0}{b}\right)}{\pi^2 \left(\frac{n^2}{a^2} + \frac{m^2}{b^2}\right) - k^2} \right] \quad (16)$$

The Sinc-Galerkin method is applied to solve the BVP. The number of terms used in the Sinc expansion (size of the basis) in both the  $x$  and  $y$ -directions are the same (as the solution is symmetric) and equal to 8 uniformly spaced values between  $M = 12$  and  $M = 36$ . This range allows us to increase the mesh density by up to a factor of 3. Similarly, we configure a typical direct BEM implementation to use a range of 4 to 12 constant elements per unit length (also a factor of 3) to solve the same problem and compare the results. We also vary the frequency (and hence the wave number  $k$ ). We test 4 frequencies in the range 20 Hz to 2000 Hz. The lower limit is the lowest audible frequency and the upper limit chosen so that the plots do not contain too many high order modes making them difficult to read. The analytical solution (crefeq:AnalHelmGF) is evaluated at each of the four frequencies truncating the series after 50 terms. The Sinc-Galerkin results for an expansion of  $2M + 1 = 65$  and the BEM for 44 elements (12 elements per unit length) are both compared to the analytical solution at the tested frequencies in Figure 1. All plots use the same colour scale.

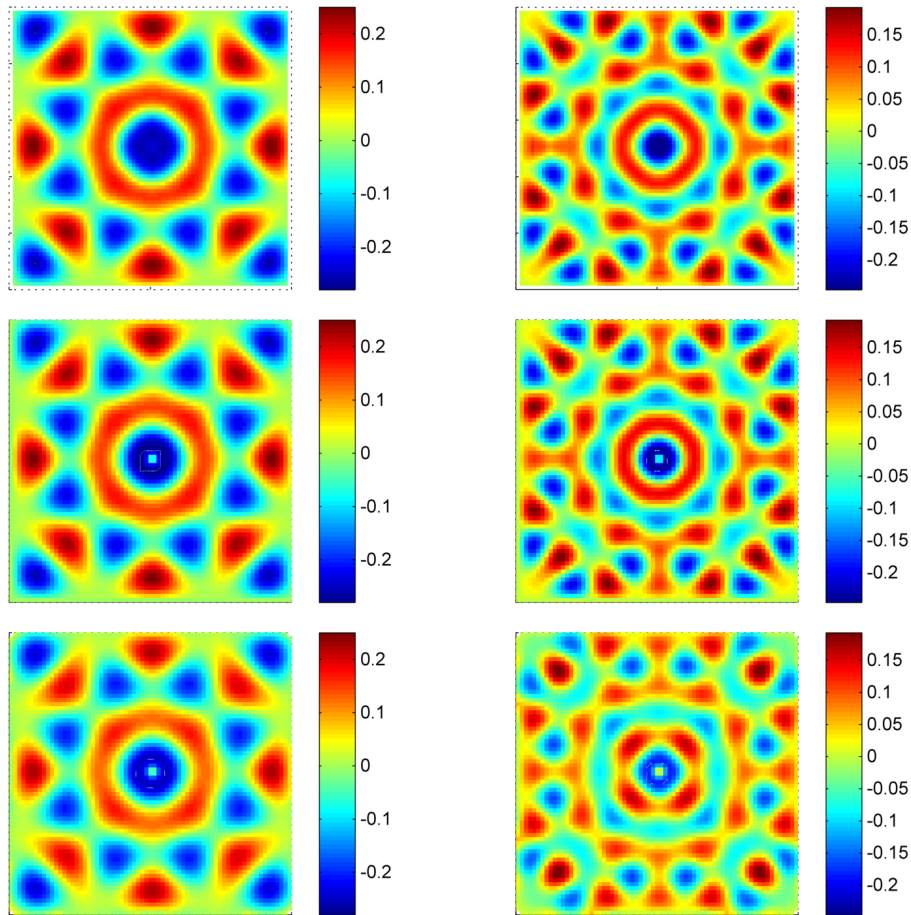
Figure 1 illustrates that the analytical solution behaves as expected. The characteristic singularity of the Green's function at the centre of the point source is visible and the homogeneous Dirichlet boundary conditions are met. As the frequency is increased the higher harmonics of the allowable modes appear which is expected to put increased demands on the ability of the numerical schemes to

resolve the solution. By comparing the Sinc-Galerkin solution to the analytical solution, we see that the singularity is only captured up to a point, with the precision of the Sinc-based approximation in the immediate vicinity of the source point being lost. This is the principle source of error when using the Sinc-Galerkin to solve our class of BVP. This may be attributed to the uneven distribution of Sinc mesh points: our source is located in the centre of the region under consideration. This coincides with the region most sparsely populated with mesh nodes. Therefore, it is expected that steep gradients are difficult to represent in this region. In addition, the peak of the Sinc function has a value of unity and hence to capture a singularity requires a large coefficient which would impact the contribution of this function over the whole of the domain. The resulting behaviour is, therefore, a trade-off between overall accuracy and the ability to capture the singularity. If the method were included as part of a domain decomposition approach to the problem, the sub-domain boundaries could be defined such that the singularity is situated on the boundary. In this case, the exponential convergence of the method could be restored. Furthermore, although the BEM results indicate that the BEM captures the singularity more precisely than the Sinc-Galerkin method, there is evidence of a loss of definition in Figure 1b at the peaks and troughs at the higher frequencies tested. Therefore, qualitatively, the Sinc-Galerkin captures the *general* behaviour of the solution with a higher degree of fidelity than the BEM, the latter demonstrating a notable resolution-driven sensitivity to frequency. From both the Sinc-Galerkin and BEM results, we also note that the boundary conditions are accurately satisfied by both methods: the BEM allows the boundary conditions to be specified precisely as in input to the method and the nature of the Sinc function itself means it decays to zero at the edge of the domain.



(a)  $f=20$  (left column) and  $f=680$  (right column)

We compare the execution time and the relative error in all cases (Figure 2a (log scale) and Figure 2b). For most of the mesh densities tested, the Sinc-Galerkin method performs reasonably well with the mean relative error remaining less than 15%. The boundary element method sees a reduction in error with mesh density more steeply than the Sinc-Galerkin method with a 3 fold increase in the mesh density reducing the error to below 1% for the lowest two frequencies. When

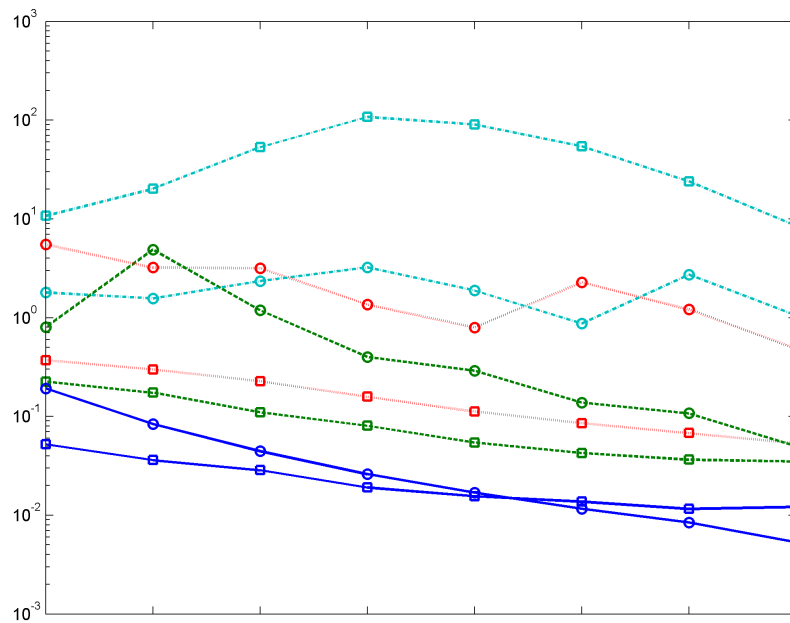
(b)  $f=1340$  (left column) and  $f=2000$  (right column)Figure 1 – Results for the BEM  $n=12$  (bottom row), analytical expression Equation (16) (middle row) and Sinc-Galerkin  $M=32$  (top row) for a source centred in the unit square

using BEM the largest errors are typically found near the boundary. Although a large relative error at these points is expected, as the analytical solution tends to zero in these regions, the absolute error is also larger than the Sinc-Galerkin method in these regions. Due to the nature of internal point evaluation for the BEM, singular collocation points on the boundary are close and sensitive to numerical inaccuracies.

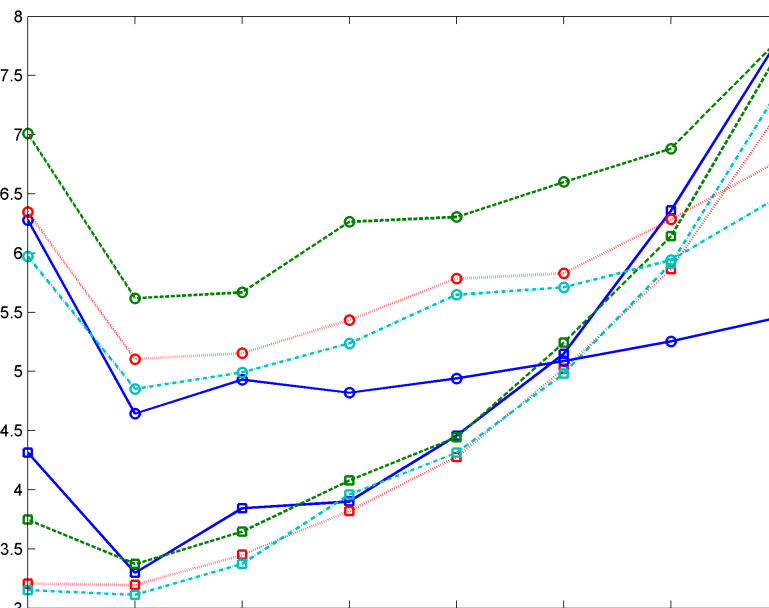
The sensitivity to frequency of the BEM is more dramatic than the Sinc-Galerkin method. The Sinc-Galerkin method performs poorly at the highest frequency tested initially due to the basis being of insufficient size to ensure the expansion converges to a suitable degree as to accurately represent the field. As the number of terms in the expansion is increased, the error begins to reduce. Although at the highest mesh density tested the relative error is still large, it is driven by a combination of localised error in the vicinity of the singularity, specifically at the ‘tip’, and small errors in regions where the analytical representation is near zero resulting in large relative errors. Figure 1 supports this assertion.

From Figure 2a, the convergence rates for both the BEM and the Sinc-Galerkin are different, with the BEM converging quicker with a trebling of the mesh density compared with the Sinc-Galerkin. However, despite the presence of a domain singularity, the lines are roughly linear which suggests an exponential variation (logarithmic scale).

With respect to execution time, the Sinc-Galerkin still achieves comparable accuracy to the BEM in most of the combinations tested while taking less time to execute (Figure 2b). Specifically at lower mesh resolutions, it can be up to 2.5 times longer to use the BEM over the Sinc-Galerkin. This is due to the simplicity of the sinc quadrature rule which avoids expensive numerical integration. As the mesh density increases, however, the time taken scales non-linearly for the Sinc-Galerkin and roughly linearly for the BEM although the latter with an increased frequency dependence.



(a) f=20 (solid blue), f=680 (dashed green), f=1340 (dotted red), f=2000 (dot-dash cyan).



(b) f=20 (solid blue), f=680 (dashed green), f=1340 (dotted red), f=2000 (dot-dash cyan).

Figure 2 – Relative error (top) and execution time in seconds (bottom) for Sinc-Galerkin (squares) and BEM (circles) for the range of mesh densities tested (horizontal axis) for a centred source. f=20 (solid blue), f=680 (dashed green), f=1340 (dotted red), f=2000 (dot-dash cyan).

## 6. CONCLUSIONS

We have applied the 2D Sinc-Galerkin method to numerically evaluate the Green's function for the Helmholtz equation in a rectangular patch subject to homogeneous Dirichlet boundary conditions. The results for a range of frequencies and mesh densities have been compared to a direct BEM implementation both qualitatively and quantitatively in terms of relative error and execution time. The results illustrate that increasing the basis size of the Sinc-Galerkin method by a factor of 3 results in a slower convergence than is achieved when increasing the number of boundary elements by the same factor. Furthermore, unlike the BEM, the domain singularity is not completely captured in the immediate vicinity of the point itself. However, a suitable means of domain decomposition could move this singularity onto the boundary and exponential convergence of the method would be restored. Overall representation of the solution is accurate, robust and quick to evaluate when compared with the BEM. Only for the largest basis size tested did the time taken to execute storage requirements exceed those of the BEM. The efficiency of the method may be attributed to the lack of a requirement for expensive numerical integration. Furthermore, despite the domain singularity, which reduces the potency of the exponential convergence of the Sinc-Galerkin method, for most combinations of mesh density and frequency tested, the Sinc-Galerkin achieves lower relative errors compared to the BEM. The formulation presented may be easily extended to 3D spatial and temporal variations.

### Acknowledgements

The work was completed as part of the first author's doctorate degree, supervised by the second author and funded by the alumni of the University of Manchester through Your Manchester Fund. This material has subsequently been expanded upon and submitted to the Journal of Applied Maths and Physics (ZAMP).

### REFERENCES

1. Wang M, Freund JB, Lele SK. Computational prediction of flow-generated sound. *Annual Review of Fluid Mechanics*. 2006;38(1):483–512.
2. Howe MS. *Theory of Vortex Sound*. Cambridge: Cambridge University Press; 2003.
3. Stenger F. A 'Sinc-Galerkin' method of solution of boundary value problems. *Mathematics of Computation*. 1979;33(145):85–109.
4. Wu X, Li C, Kong W. A Sinc-collocation method with boundary treatment for two-dimensional elliptic boundary value problems. *Journal of Computational and Applied Mathematics*. 2006;196(1):58–69.
5. Bowers K, Lund J. Numerical Solution of Singular Poisson Problems via the Sinc-Galerkin Method. *SIAM Journal on Numerical Analysis*. 1987;24(1):36–51.
6. Mohsen A, El-Gamel M. On the Galerkin and collocation methods for two-point boundary value problems using sinc bases. *Computers & Mathematics with Applications*. 2008;56(4):930–941.
7. Lund J, Bowers KL. *Sinc Methods for Quadrature and Differential Equations*. Philadelphia: Society for Industrial and Applied Mathematics; 1992.
8. McArthur KM, Bowers KL, Lund J. The Sinc method in multiple space dimensions: Model problems. *Numerische Mathematik*. 1990;56(8):789–816. Available from: <http://dx.doi.org/10.1007/BF01405289>.
9. Lybeck NJ, Bowers KL. Domain decomposition in conjunction with sinc methods for Poisson's equation. *Numerical Methods for Partial Differential Equations*. 1996;12(4):461–487.
10. Koonprasert S, Bowers KL. The fully Sinc-Galerkin method for time-dependent boundary conditions. *Numerical Methods for Partial Differential Equations*. 2004;20(4):494–526.
11. Mueller JL, Shores TS. A new sinc-galerkin method for convection-diffusion equations with mixed boundary conditions. *Computers & Mathematics with Applications*. 2004;47(4–5):803–822.
12. Selvadurai APS. *Partial Differential Equations in Mechanics: Vol. 1 Fundamentals, Laplace's equation, diffusion equation, wave equation.. vol. 1*. New York: Springer-Verlag; 2000.